Phase transition in orthorhombic perovskite $Sm_{1-x}Lu_xMnO_3$: Evidenced by the emergence of ferroelectric polarization

Na Zhang,[1,2] Shuai Dong,[3,a)] Meifeng Liu,[2] Zhaoming Fu,[1] Fanggao Chang,[1] and Jun-Ming Liu[2,b)]
[1]*Henan Province Key Laboratory of Photovoltaic Materials, Henan Normal University, Xinxiang 453007, China*
[2]*Laboratory of Solid State Microstructures, Nanjing University, Nanjing 210093, China*
[3]*Department of Physics, Southeast University, Nanjing 211189, China*

(Presented 7 November 2014; received 21 September 2014; accepted 23 November 2014; published online 8 April 2015)

A series of polycrystalline orthorhombic manganites $Sm_{1-x}Lu_xMnO_3$ have been synthesized in order to study the magnetism-induced ferroelectricity. Detailed measurements of the magnetic and electric properties of $Sm_{1-x}Lu_xMnO_3$ ($0 \le x \le 0.3$) compounds have been performed. The obtained Mn-O-Mn bond angle and the Néel temperature decrease with increasing x, indicating the strengthened frustration of original A-type antiferromagnetic (A-AFM) order of Mn spins. For lower x concentrations, no ferroelectricity is detected, implying the stability of the A-AFM ordering. Further increasing x, a dielectric anomaly begins to develop at 28 K since $x = 0.15$ which is not observed in $SmMnO_3$. Coinciding with this dielectric anomaly, a ferroelectric polarization emerges, implying the multiferroicity. For intermediate compositions, a possible complex phase separation exists. © *2015 AIP Publishing LLC*. [http://dx.doi.org/10.1063/1.4916555]

Nowadays, multiferroics with coexisting magnetic and ferroelectric (FE) orders have attracted increasing interests for their potential applications associated with the magnetoelectric (ME) coupling.[1–3] However, due to the exclusion between the magnetism and ferroelectricity, the direct combination of these two orders in one single phase material is quite challenge.[3,4] Thus, alternative approaches have been adapted to explore the so-called multiferroics.[1–3] Recently, limited multiferroic materials have been discovered, which can be classified into two types: the type-I multiferroics in which the magnetism and ferroelectricity come from different origins and thus have weak mutual couplings;[5] the type-II multiferroics in which the ferroelectric polarization is intrinsically originated from and thus strongly coupled with the particular magnetic structures, e.g., noncollinear spiral spin order (SSO) and E-type antiferromagnetic (E-AFM) order.[1–3,6] Due to the special origins of ferroelectric polarizations, the coupling between magnetism and ferroelectricity in the type-II multiferroics is intrinsic. The external magnetic field can not only modulate the magnitude of polarization but also even flip the direction of polarization in these materials.[7,8] In this sense, the type-II multiferroics contain more physics and will be also important in the future spintronic applications.

The orthorhombic ABO_3-type manganites $RMnO_3$ (R is a small size trivalent rare-earth ion), with strong competition between charge, spin, and orbital degrees of freedom and complex interactions, contains some typical type-II multiferroics.[9] When reducing the ionic size of R, the magnetic ground state changes from the A-type AFM (A-AFM) spin order to the multiferroic SSO and then to the multiferroic E-AFM. However, the multiferroic $RMnO_3$ samples are rare, due to the fact that the specific spin orders only exist in $RMnO_3$ with very small ionic size of R, which's orthorhombic crystal structure is unstable against the hexagonal one.

A simple way to reduce the A-site ionic size of $RMnO_3$ is through substituting the A-site ions with smaller rare-earth ions; then the Mn-O-Mn bond angles can be reduced to favor the SSO or E-AFM order. In fact, the magnetic phase transition from the A-AFM to SSO order and then a finite polarization P have been observed in both the $Nd_{1-x}Y_xMnO_3$ and $Eu_{1-x}Y_xMnO_3$ systems.[10–12] Based on these results, it is reasonable to believe that the A-AFM $SmMnO_3$, lying between the $NdMnO_3$ and $EuMnO_3$,[13] can also be modified into multiferroic phase through the A-site elements substitution.

Although lacking of the ferroelectricity, the A-AFM $SmMnO_3$ possesses weak ferromagnetism[14] and also exhibits some peculiar phenomena, such as the temperature-induced magnetization reversal and resultant negative magnetization in weak magnetic fields.[15] This phenomenon sticks the label of Néel's N-type ferrimagneticity[16] and is ascribed to the antiparallel coupling between Sm's 4*f* moments and canted Mn's 3*d* moments.[15] Additionally, the recently observed distinct magnetocapacitive effects also make the $SmMnO_3$ distinct from other $RMnO_3$.[17] In the present work, we select the smallest ionic radius rare earth Lu^{3+} ($r = 86.1$ pm) to partial substitute the A-site Sm^{3+} ($r = 95.8$ pm)[18] to effectively enhance the $GdFeO_3$-type distortion and then transform the $SmMnO_3$ into the frustration spin structure to pursuit the multiferroicity.[19]

We prepared a series of polycrystalline orthorhombic $Sm_{1-x}Lu_xMnO_3$ ($0 \le x \le 0.5$) by the sol-gel method. Sm_2O_3 and Lu_2O_3 powder in stoichiometric ratio was dissolved in

a)Electronic mail: sdong@seu.edu.cn.
b)Electronic mail: liujm@nju.edu.cn.

dilute nitric acid, then $Mn(CH_3COO)_2{\cdot}4H_2O$ and an equal amount of ethylene glycol were added with continuous stirring. The solution was treated in the same way as reported,[20] and the obtained xerogel precursor was grinded and heated in air at 800 °C for 24 h. The resultant powders were pressed into pellets and sintered in air at 850 °C for additional 24 h.

Phase purity in all samples was identified by X-ray diffraction (XRD) with Cu $K\alpha$ radiation at room temperature. The static (DC) magnetization (M) and specific-heat (C) in response to temperature (T) were probed employing the Superconducting Quantum interference device (SQUID) and Physical Properties measurement system (PPMS), respectively. For electric measurements, gold contacts were painted onto the pellets. The dielectric constant (ε) was measured as a function of temperature at 10 kHz using an Agilent 4294A impedance analyzer, while polarization P was obtained by using the pyroelectric current method with the Keithley 6514A electrometer plus careful exclusion of other possible contributions such as those from the de-trapped charges. At last, P was evaluated from the measured pyroelectric current. Details of such measurement and data processing were reported in an earlier work.[21]

First, the crystallinity and structure of the as-prepared samples are checked. Schematic drawing of the lattice structure of $SmMnO_3$ and the probed XRD patterns for the $Sm_{1-x}Lu_xMnO_3$ ($0 \le x \le 0.5$) samples at room temperature are shown in Figs. 1(a) and 1(b), respectively. A careful check of these data in assistance with the standard JPCD database reveals that all the samples are in single phase and crystallize with the orthorhombic structure (space group *Pnma*). Traces of impurity phases could be detected in samples only when $x > 0.5$, indicating that the single-phase orthorhombic structure in $Sm_{1-x}Lu_xMnO_3$ synthesized in our experiments can be maintained up to $x = 0.5$. The substitution of Sm with Lu effectively modifies the crystal structure of $Sm_{1-x}Lu_xMnO_3$ compared to $SmMnO_3$. As shown in the inset of Fig. 1(b), a continuous and almost linear shifting of these reflections towards the high angle side is identified, suggesting the lattice shrinking with increasing x. Noting that the ionic radius value of Lu^{3+} is much smaller than that of Sm^{3+},[18] this variation is under expectation.

In order to identify details of the crystal structural, we perform high-precision Rietveld refining of the XRD data obtained at room temperature in the *Pnma* space group, which can be maintained even at low temperature.[22] With increasing Lu content, the lattice contracts linearly along the b and c directions, while leaving the a almost constant, as shown in Fig. 1(c). Accompanying this anisotropic change in the lattice, linearly reduction in volume and Mn-O_1-Mn bond angle (ϕ) with increasing x are observed, as displayed in Fig. 1(d). It is revealed that the decreased ϕ will significantly modulate the strength of the superexchange interaction between Mn ions and lead to the transformation from the original A-AFM order into frustrated spin structures.[13]

Subsequently, the evolution of the magnetic behaviors upon Lu-substitution is studied. The x-dependences of $M(T)$ data, shown in Figs. 2(a) and 2(b), were obtained under the "zero-field-cooling" (ZFC) and "field-cooling" (FC) conditions with a weak magnetic field $H \sim 100$ Oe. For pure $SmMnO_3$ [Fig. 2(a)], the ZFC and FC curves diverge at $T_N = 59$ K. Below T_N, an obvious rise of M is observed, measured under the FC condition, which is connected with the emergence of canted A-AFM order of Mn^{3+} moments.[17] Further cooling down the sample, the M (FC) passes through a broad maximum around 25 K and turns to zero around $T_{comp} = 6$ K. The zero value of M (FC) is believed to be resulting from the balance between the net ferromagnetic moment of canted Mn^{3+} spins and the oppositely oriented Sm^{3+} magnetic moments.[22,23] With further decreasing T below T_{comp}, M (FC) becomes negative, which is also attributed to the antiparallel orientation of the canted Mn^{3+} moments and increased Sm^{3+} moments coupled by the Sm-Mn exchange interactions.[24] As for the Lu substituted compounds, the T_N decreases since the size of R is reduced, indicating the strengthened frustration of original magnetic ordering.[11,13,25]

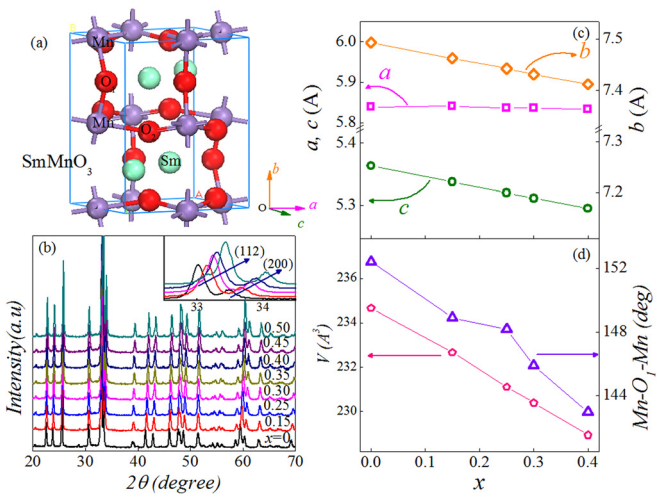

FIG. 1. (a) Sketch of the crystal structure of $SmMnO_3$. (b) Room temperature XRD patterns of $Sm_{1-x}Lu_xMnO_3$ ($0 \le x \le 0.5$). The inset shows the shifting of the (110) and (002) peaks with increasing $x = 0$, 0.15, 0.3, 0.4, and 0.5 from bottom to up. (c) The obtained lattice parameters of a, b, and c as a function of x. (d) The evaluated lattice volume V and Mn-O_1-Mn bond angle as a function of x.

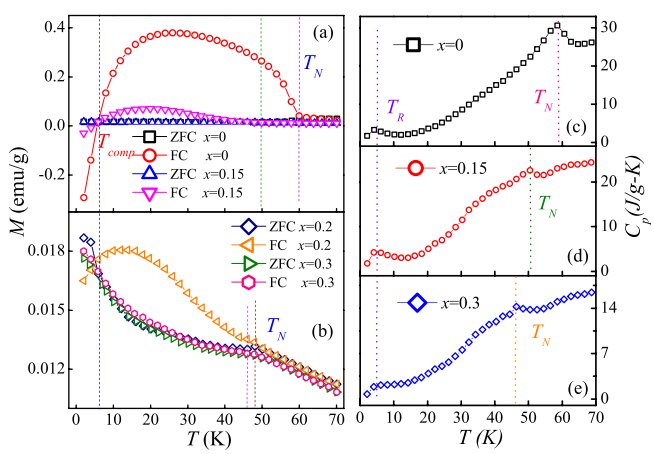

FIG. 2. The evolution of the magnetism and heat capacity of $Sm_{1-x}Lu_xMnO_3$ ($0 \le x \le 0.3$) samples. Measured M-T curves under the ZFC and FC conditions for (a) $x = 0$ and 0.15 and (b) 0.2 and 0.3 samples. Measured C-T plots for (c) $x = 0$, (d) $x = 0.15$, and (e) $x = 0.3$, respectively.

Furthermore, as shown in Figs. 2(a) and 2(b), the value of M of $Sm_{1-x}Lu_xMnO_3$ compounds is suppressed to one magnitude lower than $SmMnO_3$, which can be attributed to the suppression of the canted Mn^{3+} moments by the A-site Lu substitution.[26] In additional, the value of M no longer becomes negative even down to the lowest T (2 K) for those $x \geq 0.2$ compositions, as shown in Fig. 2(b), implying the destruction of the polarized Sm^{3+} moment under heavy nonmagnetic Lu^{3+} dilution.

In order to further characterize the magnetic ordering of $Sm_{1-x}Lu_xMnO_3$ compositions, T-dependent specific heat measurements were carried out, and the results for representative samples are displayed in Figs. 2(c)–2(e). According to these C-T curves, we were able to determine T_N's independently and compare these values to the aforementioned magnetic measurements. The measured C-T curve for pure $SmMnO_3$ sample is shown in Fig. 2(c). The λ-shaped anomaly observed at $T_N = 59$ K coincides well with the steep rise of M, which can be assigned to the A-AFM ordering of Mn spins.[13,22,26] The broad peak detected around $T_R = 4$ K is related to the magnetic ordering of Sm moments.[13,22,26] In excellent agreement with the M-T data, the measured C-T curves for $Sm_{1-x}Lu_xMnO_3$ samples indicate that the Lu-substitution results in the downshift of T_N with increasing x. Otherwise, the broad peak of T_R disappears when $x \geq 0.2$, suggesting the disruption of ordering of Sm moments.[26] Additionally, the Lu-substitution also slightly modulates the critical point of T_N.

In $RMnO_3$, the decrease in T_N is closely related with the reduction of ϕ. The decreased ϕ and staggered orbital ordering will lead to a competition between the ferromagnetic nearest-neighbor (J_1) and antiferromagnetic next-nearest-neighbor (J_2) superexchange interactions between Mn^{3+}'s, and finally bring forward the magnetic phase transition from the A-AFM order to the SSO.[13,19] Therefore, enlarged crystal structural distortion is naturally expected in $Sm_{1-x}Lu_xMnO_3$ system. However, the second magnetic phase transition of Mn moment,[26] which is the indication of the transition to the SSO, has not been detected in our C-T curves of $Sm_{1-x}Lu_xMnO_3$ samples. Even though, the Lu substitution induced FE phase transition is indeed occurred, as reflected in our dielectric and ferroelectric properties measurements.

It is reported that the dielectric constant of pure $SmMnO_3$ decreases monotonously with decreasing temperature, and no clear anomaly was observed over the whole T-range.[27] Upon Lu substitution, the ε-T curves of $Sm_{1-x}Lu_xMnO_3$ samples reveal a well defined peak below T_N, e.g., around 28 K for the $x = 0.15$ sample, as shown in Fig. 3, which is a hint for ferroelectric transition. Indeed, the pyroelectric measurement of the $Sm_{0.85}Lu_{0.15}MnO_3$ sample reveals that a weak ferroelectric polarization (P) with its largest value $\sim 2.4\ \mu C/m^2$ emerges below $T_{FE} = 28$ K, providing further evidence for the existence of a second magnetic phase transition of Mn spins. In other words, the presence of ferroelectricity induced by magnetism implies the magnetic multiferroic nature of $Sm_{0.85}Lu_{0.15}MnO_3$ sample. At $x = 0.2$ concentration, the largest value of P is effectively enhanced up to 8.9 $\mu C/m^2$. Further increasing x, the dielectric peak of $Sm_{1-x}Lu_xMnO_3$ gradually moves down to

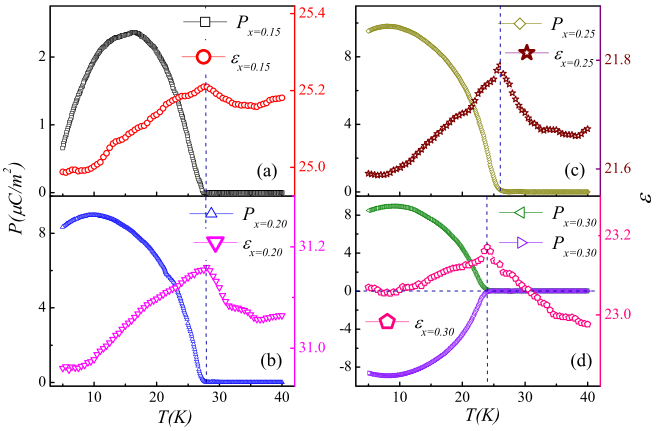

FIG. 3. Measured dielectric constant $\varepsilon(T)$ and pyroelectric polarization $P(T)$ curves for (a) $x = 0.15$, (b) $x = 0.2$, (c) $x = 0.25$, and (d) $x = 0.3$, respectively.

lower temperature, while the largest values of P are approximately unchanged for all $x \geq 0.2$ compositions as indicated in Fig. 3. Furthermore, one should note that these values of P are much smaller compared to the well oriented single crystal $Nd_{1-x}Y_xMnO_3$ and $Sm_{1-x}Y_xMnO_3$,[11,26] which may be attributed to the random grain directions in the polycrystalline samples.[28] Additionally, the grain boundaries and smaller grain size, resulting from the low crystallization temperature used in the sol-gel sintering method, will not only prevent the formation of the long-range FE order but also can lead to the clamping of domain walls, causing a smaller macroscopic P.[29,30] Moreover, accompanied with the smaller grain size, the extrinsic contributions of grain boundaries, defects, and space charges to ε are non-negligible, which makes the comparison of the absolute values of ε between different samples meaningless. Qualitatively, the emergence of P suggests the unambiguous multiferroicity in $Sm_{1-x}Lu_xMnO_3$.

Aiming to get a comprehensive understanding of Lu substitution effects on the multiferroic properties of $SmMnO_3$, a T-x magnetic phase diagram of the $Sm_{1-x}Lu_xMnO_3$ series has been established for x varying from 0 to 0.3, based on above experimental results. As shown in Fig. 4, in general, the substantial impact of Lu's partial substitution for Sm is clearly reflected by the decreased T_N and the emergence of ferroelectricity.

According to our previous theoretical prediction, the lattice contraction induced by decreasing the average rare earth radii $\langle r_A \rangle$ of $RMnO_3$ will effectively enlarge the cooperative rotation and tilting of the MnO_6 octahedra characterized by the decrease of ϕ, which will drive the system to undergo a phase transition from the A-AFM phase into a SSO phase.[13,19] The space inversion symmetry is broken by the SSO of Mn spins, leading to the emergence of spontaneous polarization. The as-generated polarization can be described as $P \sim A e_{ij} \langle S_i \times S_j \rangle$,[19,28,31,32] where e_{ij} denotes the unit vector connecting the two neighbor spins (S_i and S_j) and coefficient A is mainly relevant to the spin-orbit coupling.

For the $Sm_{1-x}Lu_xMnO_3$ system, due to the significant icon radius difference between Sm^{3+} and Lu^{3+}, reduced average ionic radius $\langle r_A \rangle$ of the A site and obvious lattice shrinkage have been confirmed, as shown in Figs. 1 and 4.

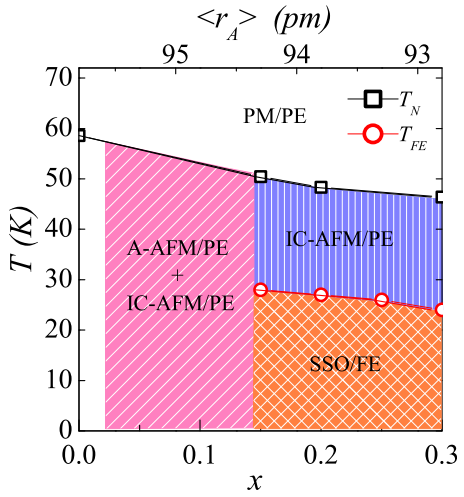

FIG. 4. Magnetic phase diagram for the $Sm_{1-x}Lu_xMnO_3$ ($0 \le x \le 0.3$) system. The T_N and T_{FE} represent the Néel temperature and the ferroelectric Curie temperature of $Sm_{1-x}Lu_xMnO_3$ compositions, obtained from the specific heat and ferroelectric measurements, respectively. The PM, IC, and AFM denote the paramagnetic, incommensurate, and antiferromagnetic spin orders, respectively. The PE and FE represent the paraelectric and ferroelectric phase, respectively. The shade areas are guide for eyes.

The decreased ϕ accompanied with the reduction in $\langle r_A \rangle$ frustrates the original A-AFM order of $SmMnO_3$ and leads to the decrease of T_N of $Sm_{1-x}Lu_xMnO_3$ samples.[1,13,19] With strengthened magnetic frustration, the magnetic ground state of $Sm_{1-x}Lu_xMnO_3$ will transform into noncollinear SSO,[19] as evidenced by the emergence of P in $x \ge 0.15$ compositions. Additionally, due to the significant contrast in size and magnetic properties between Sm^{3+} and Lu^{3+}, the A-site quenching disorder will be introduced into the $Sm_{1-x}Lu_xMnO_3$ compounds, which may accelerate the disruption of original long-range ordering of Mn^{3+} moments that thus in turn boost the formation of SSO.[10] Furthermore, it has been revealed that due to the quenching disorder effect, the phase transition between the A-AFM and SSO is not continuous but is separated by a complex phase separation state.[10,11,31–34] Such coexistence of A-AFM order and no-FE incommensurate (IC) order is conceivable to emerge around our $x = 0.1$ concentrations.

Honestly, direct measurements of the magnetic phase evolution of $Sm_{1-x}Lu_xMnO_3$ system can be done via the neutron-diffraction experiments, which may provide more intuitive evidences. Even though, the ultimate interest of our work is the possibility of fine tuning of magnetic interactions and the multiferroicity in $RMnO_3$ compositions. In this sense, our simple macroscopic measurements have already revealed the phase evolution process of $Sm_{1-x}Lu_xMnO_3$.

In summary, polycrystalline $Sm_{1-x}Lu_xMnO_3$ samples have been prepared to investigate the effect of A-site substitution on magnetic transitions and ferroelectric properties. It has been demonstrated that the partial substitution of Sm with Lu in $SmMnO_3$ is indeed an effective tool to modulate the magnetic structure and then induce multiferroic properties. We argue that the increased tilting angles of the MnO_6 octahedra and the quenched disorder, as a result of the significant mismatch between Sm^{3+} and Lu^{3+}, cause an obvious modulation on the complex exchange interaction between Mn spins, which changes the original canted A-type antiferromagnetism into the multiferroic spiral spin order, through the complex phase coexistence phase. In addition, the nonmagnetic Lu^{3+} also suppresses the magnetism of Sm^{3+} and its interaction with Mn's moments.

This work was supported by the Natural Science Foundation of China (11234005, 51322206, U1204111, and 11247012), the Specialized Research Fund for the Doctoral Program of Higher Education, and the open project of Nanjing National Laboratory of Microstructures (2013M531677, 2011040 and M26002).

[1]S.-W. Cheong *et al.*, Nat. Mater. **6**, 13 (2007).
[2]K. F. Wang *et al.*, Mod. Phys. Lett. B **26**, 1230004 (2012).
[3]M. Fiebig, J. Phys. D: Appl. Phys. **38**, R123 (2005).
[4]N. A. Hill, J. Phys. Chem. B **104**, 6694 (2000).
[5]D. Khomskii, Physics **2**, 20 (2009); G. Catalan *et al.*, Adv. Mater. **21**, 2463 (2009).
[6]Y. Tokura, Science **312**, 1481 (2006); W. Eerenstein *et al.*, Nature (London) **442**, 759 (2006).
[7]T. Kimura *et al.*, Phys. Rev. B **71**, 224425 (2005).
[8]R. Feyerherm *et al.*, Phys. Rev. B **79**, 134426 (2009).
[9]J. B. Goodenough, Rep. Prog. Phys. **67**, 1915 (2004).
[10]S. Landsgesell *et al.*, Phys. Rev. B **80**, 014412 (2009).
[11]S. Landsgesell *et al.*, Phys. Rev. B **86**, 054429 (2012).
[12]J. Hemberger *et al.*, Phys. Rev. B **75**, 035118 (2007).
[13]T. Kimura *et al.*, Phys. Rev. B **68**, 060403(R) (2003).
[14]V. Skumryev *et al.*, Eur. Phys. J. B **11**, 401 (1999).
[15]V. Yu. Ivanov *et al.*, Phys. Status Solidi B **236**, 445 (2003).
[16]L. Néel, Ann. Phys. (Paris) **3**, 137 (1948).
[17]J.-S. Jung *et al.*, Phys. Rev. B **82**, 212403 (2010).
[18]R. D. Shannon, Acta Cryst., Sect. A: Cryst. Phys., Diffr., Theor. Gen. Crystallogr. **32**, 751 (1976).
[19]S. Dong *et al.*, Phys. Rev. B **78**, 155121 (2008).
[20]K. S. Shankar *et al.*, Solid State Commun. **129**, 479 (2004).
[21]N. Zhang *et al.*, Appl. Phys. Lett. **99**, 102509 (2011).
[22]J.-G. Cheng *et al.*, Phys. Rev. B **84**, 104415 (2011).
[23]S. A. Uporov *et al.*, J. Mater. Sci. **48**, 7673 (2013).
[24]A. A. Mukhin *et al.*, J. Magn. Magn. Mater. **272**, 96 (2004).
[25]T. Kimura *et al.*, Phys. Rev. B **67**, 180401(R) (2003).
[26]D. O'Flynn *et al.*, Phys. Rev. B **83**, 174426 (2011).
[27]D. O'Flynn *et al.*, J. Phys.: Conf. Ser. **200**, 012149 (2010).
[28]S. Ishiwata *et al.*, Phys. Rev. B **81**, 100411(R) (2010).
[29]Z. Zhao *et al.*, Phys. Rev. B **70**, 024107 (2004).
[30]S. S. Rao *et al.*, Phys. Rev. B **74**, 144416 (2006).
[31]M. Mostovoy, Phys. Rev. Lett. **96**, 067601 (2006).
[32]H. Katsura *et al.*, Phys. Rev. Lett. **95**, 057205 (2005).
[33]E. Dagotto *et al.*, Phys. Rep. **344**, 1 (2001).
[34]J. Burgy *et al.*, Phys. Rev. Lett. **87**, 277202 (2001).